Quantifying Soil Carbon Accumulation in Alaskan Terrestrial Ecosystems during the Last 15,000 Years

Sirui Wang[1], Qianlai Zhuang[1,2*], Zicheng Yu[3]

[1]Department of Earth, Atmospheric, and Planetary Sciences, Purdue University, West Lafayette, Indiana, 47907

[2]Department of Agronomy, Purdue University, West Lafayette, IN 47907

[3]Department of Earth and Environmental Sciences, Lehigh University, Bethlehem, PA 18015

Correspondence to: qzhuang@purdue.edu

Abstract: Northern high latitudes contain large amounts of soil organic carbon (SOC), in which Alaskan terrestrial ecosystems account for a substantial proportion. In this study, the SOC accumulation in Alaskan terrestrial ecosystems over the last 15,000 years was simulated using a process-based biogeochemistry model for both peatland and non-peatland ecosystems. Comparable with the previous estimates of 25-70 Pg C in peatland and 13-22 Pg C in non-peatland soils within 1-m depth in Alaska, our model estimated a total SOC of 36-63 Pg C at present, including 27-48 Pg C in peatland soils and 9-15 Pg C in non-peatland soils. Current vegetation stored 2.5-3.7 Pg C in Alaska with 0.3-0.6 Pg C in peatlands and 2.2-3.1 Pg C in non-peatlands. The simulated average rate of peat C accumulation was 2.3 Tg C yr^{-1} with a peak value of 5.1 Tg C yr^{-1} during the Holocene Thermal Maximum (HTM) in the early Holocene, four folds higher than the average rate of 1.4 Tg C yr^{-1} over the rest of the Holocene. The SOC accumulation slowed down, or even ceased, during the neoglacial climate cooling after the mid-Holocene, but increased again in the 20^{th} century. The model-estimated peat depths ranged from 1.1 to 2.7 m, similar to the field-based estimate of 2.29 m for the region. We found that the changes in vegetation and their distributions were the main factors to determine the spatial variations of SOC accumulation during different time periods. Warmer summer temperature and stronger radiation seasonality, along with higher precipitation in the HTM and the 20^{th} century might have resulted in the extensive peatland expansion and carbon accumulation.

Keywords: Carbon, Peatlands, Alaska, Modelling, Climate

1. Introduction

Global surface air temperature has been increasing since the middle of the 19th century (Jones and Mogberg, 2003; Manabe and Wetherald, 1980, 1986). Since 1970, the warming trend has accelerated at a rate of 0.35 ℃ per decade in northern high latitudes (Euskirchen et al., 2007; McGuire et al., 2009). It is predicted that the warming will continue in the next 100 years (Arctic Climate Impact Assessment 2005; Intergovernmental Panel on Climate Change (IPCC), 2013, 2014). The land surface in northern high latitudes (>45° N) occupies 22% of the global surface and stores over 40% of the global soil organic carbon (SOC) (McGuire et al., 1995; Melillo et al., 1995; McGuire and Hobbie, 1997). Specifically, the northern high latitudes were estimated to store 200-600 Pg C (1 Pg C = 10^{15} g C) in peatland soils depending on the depth considered (Gorham, 1990, 1991; Yu, 2012), 750 Pg C in non-peatland soils (within 3 m) (Schuur et al., 2008; Tarnocai et al., 2009; Hugelius et al., 2014), and additional 400 Pg C in frozen loess deposits of Siberia (Zimov et al., 2006a). Peatland area is around 40 million hectares in Alaska compared with total 350 million hectares in northern high latitudes (Kivinen and Pakarinen, 1981). Alaskan peatlands account for the most peatland area in the USA and cover at least 8% of the total land area (Bridgham et al., 2006). To date, the regional soil C and its responses to the climate change are still with large uncertainties (McGuire et al., 2009; Loisel et al., 2014).

The warming climate could increase C input to soils as litters through stimulating plant net primary productivity (NPP) (Loisel et al., 2012). However, it can also decrease the SOC by increasing soil respiration (Yu et al., 2009). Warming can also draw down the water table in peatlands by increasing evapotranspiration, resulting in higher decomposition as the aerobic respiration has a higher rate than anaerobic respiration in general (Hobbie et al., 2000). SOC accumulates where the rate of soil C input is higher than decomposition. The variation of climate may switch the role of soils between a C sink and a C source (Davidson and Janssens, 2006; Davidson et al., 2000; Jobbagy and Jackson, 2000). Unfortunately, due to the data gaps of field-measurement and uncertainties in estimating regional C stock (Yu, 2012), with limited understanding of both peatlands and non-peatlands and their responses to climate change, there is no consensus on the sink and source activities of these ecosystems (Frolking et al., 2011; Belyea, 2009; McGuire et al., 2009).

Both observation and model simulation studies have been applied to understand the long-term peat C accumulation in northern high latitudes. Most field estimations are based on series of peat-core samples (Turunen et al., 2002; Roulet et al., 2007; Yu et al., 2009; Tarnocai et al., 2009). However, those core analyses may not be adequate for estimating the regional C accumulation due to their limited spatial coverage. To date, a number of model simulations have also been carried out. For instance, Frolking et al. (2010) developed a peatland model considering the effects of plant community, hydrological dynamics and peat properties on SOC accumulation. The simulated results were compared with peat-core data. They further analyzed the contributions of different plant functional types (PFTs) to the peat C accumulation. However, this 1-D model has not been evaluated with respect to soil moisture, water-table depth, methane fluxes, and carbon and nitrogen fluxes and has not been used in large spatial-scale simulations by considering other environmental factors (e.g., temperature, vapor pressure, and radiation). In contrast, Spahni et al. (2013) used a dynamic global vegetation and land surface process model (LPX), based on LPJ (Sitch et al., 2003), imbedded with a peatland module, which considered the nitrogen feedback on plant productivity (Xu-Ri and Prentice, 2008) and plant biogeography, to simulate the SOC accumulation rates of northern peatlands. However, the model did not consider methane dynamics, which play an important role in affecting peat carbon dynamics, presumably due to its inadequate representation of ecosystem processes (Stocker et al., 2011, 2014; Kleinen et al., 2012). Furthermore, climatic effects on SOC were not fully explained. The Terrestrial Ecosystem Model (TEM) has been applied to study C and nitrogen dynamics in the Arctic (Zhuang et al., 2001, 2002, 2003, 2015; He et al., 2014). However, the model has not been calibrated and evaluated with peat-core C data, and has not been applied to investigate the regional peatland C dynamics. Building upon these efforts, recently we fully evaluated the peatland version of TEM (P-TEM) including modules of hydrology (HM), soil thermal (STM), C and nitrogen dynamics (CNDM) for both upland and peatland ecosystems (Wang et al., 2016).

Here we used the peatland-core data for various peatland ecosystems to parameterize and test P-TEM (Figure 1). The model was then used to quantify soil C accumulation of both peatland and non-peatland ecosystems across the Alaskan landscape since the last deglaciation. This study is among the first to examine the peatlands and non-peatlands C dynamics and their distributions and peat depths using core data at regional scales.

2. Methods

2.1. Overview

To conduct regional simulations of carbon accumulation for both uplands and peatlands, we first parameterized the P-TEM for representative ecosystems in Alaska. Second, we organized the regional vegetation and peatland distribution data, spatial basal age data for all peatland grid cells based on site-level soil core data, and climate data for each period during the Holocene. Finally, we conducted the regional simulations and sensitivity analysis.

2.2 Model Description

In P-TEM (Wang et al., 2016), peatland soil organic C (SOC) accumulation is determined by the difference between NPP and aerobic and anaerobic decompostion. Peatlands accumulate C where NPP is greater than decomposition, resulting in positive net ecosystem production (NEP):

$$NEP = NPP - R_H - R_{CH_4} - R_{CWM} - R_{CM} - R_{COM} \quad (1)$$

P-TEM was developed based on the Terrestrial Ecosystem Model (TEM) at a monthly step (Zhuang et al., 2003; 2015). It explicitly considers the process of aerobic decomposition (R_H) related to the variability of water-table depth; net methane emission after methane oxidation (R_{CH_4}); CO_2 emission due to methane oxidation (R_{CWM}) (Zhuang et al., 2015); CO_2 release accompanied with the methanogenesis (R_{CM}) (Tang et al., 2010; Conrad, 1999); and CO_2 release from other anaerobic processes (R_{COM}, e.g., fermentation, terminal electron acceptor (TEA) reduction) (Keller and Bridgham, 2007; Keller and Takagi, 2013). For upland soils, we only considered the heterotrohic respiration under aerobic condition (Raich, 1991). For detailed model description see Wang et al. (2016).

We modeled peatland soils as a two-layer system for hydrological module (HM) while keeping the three-layer system for upland soils (Zhuang et al., 2002). The soil layers above the lowest water table position are divided into: (1) moss (or litter) organic layer (0-10 cm); and (2) humic organic layer (10-30 cm) (Wang et al., 2016). Based on the total amount of water content within those two unsaturated layers, the actual water table depth (WTD) is estimated. The water content at each 1 cm above the water table can be then determined after solving the water balance equations (Zhuang et al., 2004).

In the STM module, the soil vertical profile is divided into four layers: (1) snowpack in winter, (2) moss (or litter) organic layer, (3) upper and (4) lower humic organic soil (Wang et al., 2016). Each of these soil layers is characterized with a distinct soil thermal conductivity and heat capacity. We used the observed water content to drive the STM (Zhuang et al., 2001).

The methane dynamics module (MDM) (Zhuang et al., 2004) considers the processes of methanogenesis, methanotrophy, and the transportation pathways including: (1) diffusion through the soil profile; (2) plant-aided transportation; and (3) ebullition. The soil temperatures calculated from STM, after interpolation into 1-cm sub-layers, are input to the MDM. The water-table depth and soil water content in the unsaturated zone for methane production and emission are obtained from HM, and NPP is calculated from the CNDM. Soil-water pH is prescribed from observed data and the root distribution determines the redox potential (Zhuang et al., 2004).

2.3 Model Parameterization

We have parameterized the key parameters of the individual modules including HM, STM, and MDM in Wang et al. (2016). The parameters in CNDM for upland soils and vegetation have been optimized in the previous studies (Zhuang et al 2002, 2003; Tang and Zhuang 2008). Here we parameterized P-TEM for peatland ecosystems using data from a moderate rich *Sphagnum* spp. open fen (APEXCON) and a *Sphagnum*-black spruce (*Picea mariana*) bog (APEXPER) (Table 1). Both are located in the Alaskan Peatland Experiment (APEX) study area, where *Picea mariana* is the only tree species above breast height in APEXPER. Three water table position manipulations were established in APEX including a control, a lowered, and a raised water table plots (Chivers et al., 2009; Turetsky et al., 2008;

Kane et al., 2010; Churchill et al., 2011). There were also several internal collapse scars that formed with thaw of surface permafrost, including a non-, an old, and a new collapse plots. APEXCON represents the control manipulation and APEXPER represents the non-collapse plot. The annual NPP and aboveground biomass at both sites have been measured in 2009. There were no belowground observations at APEX, however at a Canadian peatland, Mer Bleue, which includes *Sphagnum* spp. dominated bog (dominated by shrubs and *Sphagnum*) and pool fen (dominated by sedges and herbs and *Sphagnum*). The belowground biomass was also observed at Suurisuo mire complex, southern Finland, a sedge fen site dominated by *Carex rostrate*. We used the ratio (70%) of belowground biomass to total biomass from these two study sites to calculate the missing belowground biomass values at APEXCON and APEXPER (Table 2). We conducted 100,000 Monte Carlo ensemble simulations to calibrate the model for each site using a Bayesian approach and parameter values with the modes in their posterior distributions were selected (Tang and Zhuang, 2008, 2009).

2.4 Regional Model Input Data

The Alaskan C stock was simulated through the Holocene driven with vegetation data reconstructed for four time periods including a time period encompassing a millennial-scale warming event during the last deglaciation known as the BØlling-AllerØd at 15-11 ka (1 ka = 1000 cal yr Before Present), HTM during the early Holocene at 11-10 and 10-9 ka, and the mid- (9-5 ka) and late- Holocene (5 ka-1900 AD) (He et al., 2014). We used the modern vegetation distribution for the simulation during the period 1900-2000 AD (Figure 2). We assumed that the vegetation distribution remained static within each corresponding time period. Upland ecosystems were classified into boreal deciduous broadleaf forest, boreal evergreen needleleaf and mixed forest, alpine tundra, wet tundra; and barren lands (Table 3). By using the same vegetation distribution map, we reclassified the upland ecosystems into two peatland types including *Sphagnum* spp. poor fens (SP) dominated by tundra and *Sphagnum* spp.-black spruce (*Picea mariana*) bog/ peatland (SBP) dominated by forest ecosystems (Table 3).

Upland and peatland ecosystem distribution for each grid cell was determined using the wetland inundation data extracted from the NASA/ GISS global natural wetland dataset (Matthews and Fung, 1987). The resolution was resampled to $0.5° \times 0.5°$ from $1° \times 1°$. Given the same topography of Alaska during the Holocene, we assumed that the wetland distribution kept the same throughout the Holocene. The inundation fraction was assumed to be the same within each grid through time and the land grids not covered by peatland were treated as uplands. We calculated the total area of modern Alaskan peatlands to be 302,410 km^2, which was within the range from 132,000 km^2 (Bridgham et al., 2006) to 596,000 km^2 (Kivinen and Pakarinen, 1981). The soil water pH data were extracted from Carter and Scholes (2000), and the elevation data were derived from Zhuang et al. (2007).

Our regional simulations considered the effects of basal ages on carbon accumulation. To obtain the spatially explicit basal age data for all peatlands grid cells, we first categorized the observed basal ages of peat samples from Gorham et al. (2012) into different time periods (Figure 2). During each period, the spatial distribution of peatland basal ages was correlated with the dominated vegetation types. For instance, peatland initiations during 15-11 ka occurred in the pixels that were dominated by alpine tundra at south, northwestern, and southeastern coast. We thus used the vegetation types to estimate the peatland basal ages for all grid cells at regional scales (Table 4).

Climate data were bias-corrected from ECBilt-CLIO model output (Timm and Timmermann, 2007) to minimize the difference from CRU data (He et al., 2014). Climate fields include monthly precipitation, monthly air temperature, monthly net incoming solar radiation, and monthly vapor pressure at resolution of 2.5° × 2.5°. We used the same time-dependent forcing atmospheric carbon dioxide concentration data for model input as were used in ECBilt-CLIO transient simulations from the Taylor Dome (Timm and Timmermann, 2007). The historical climate data used for the simulation through the 20th century were monthly CRU2.0 data (Mitchell et al., 2004).

2.5 Simulations and Sensitivity Test

Simulations for pixels located on the Kenai Peninsula from 15 to 5 ka were first conducted with the parameterized model. The peat-core data from four peatlands on the Kenai Peninsula, Alaska (Jones and Yu, 2010; Yu et al., 2010) (see Wang et al. (2016) Table 3) were used to compare with the simulations. The observed data include the peat depth, bulk density of both organic and inorganic matters at 1-cm interval, and age determinations. The simulated C accumulation rates represent the actual ("true") rates at different times in the past. However, the calculated accumulation rates from peat cores are considered as "apparent" accumulation rates, as peat would continue to decompose since the time of formation until present when the measurement was made (Yu, 2012). To facilitate comparison between simulated and observed accumulation rates, we converted the simulated "true" accumulation rates to "apparent" rates, following the approach by Spahni et al. (2013). That is, we summed the annual net C accumulation over each 500-year interval and deducted the total amount of C decomposition from that time period, then dividing by 500 years.

Second, we conducted a transient regional simulation driven with monthly climatic data (Figure 3) from 15 ka to 2000 AD. The simulation was conducted assuming all grid cells were taken up by upland ecosystems to get the upland soil C spatial distributions during different time periods. We then conducted the second simulation assuming all grid cells were dominated by peatland ecosystems following Table 3 to obtain the distributions of peat SOC accumulation. Finally, we used the inundation fraction map to extract both uplands and peatlands and estimated the corresponding SOC stocks within each grid, which were then summed up to represent the Alaskan SOC stock. We also used the observed mean C content of 46.8% in peat mass and bulk density of 166 ± 76 kg m^{-3} in Alaska (Loisel et al., 2014) to estimate peat depth distribution from the simulated peat SOC density (kg C m^{-2}).

Third, we conducted a series of extra simulations to further examine how uncertain climates and vegetation distribution affect our results. We used the original forcing data as the standard scenario and the warmer (monthly temperature $+5$℃) and cooler (-5℃) as other two scenarios while keeping the rest forcing data unchanged. Similarly, we used the original forcing data as the standard scenario and the wetter (monthly precipitation $+10$ mm) and drier (-10 mm) to test the effect from precipitation. To further study if vegetation distribution has stronger effects on SOC accumulation than climate in Alaska, we simply replaced SBP with SP and replaced the upland forests with tundra at the beginning of 15 ka. We then conducted the simulation under “warmer” and “wetter” conditions simultaneously as described before while keeping the vegetation distribution unchanged.

3. Results and Discussion

3.1 Simulated Peatland Carbon Accumulation Rates at Site Level

Our paleo simulations showed a large peak of peat C accumulation rates at 11-9 ka during the HTM (Figure 4). The simulated "true" and "apparent" rates captured this primary feature in peat-core data at almost all sites (Jones and Yu, 2010; See Wang e al. (2016) Table 3 for sites details). We simulated an average of peat SOC "apparent" accumulation rate of 11.4 $\mathrm{g\ C\ m^{-2}\ yr^{-1}}$ from 15 to 5 ka, which was slightly higher than the observations at four sites (10.45 $\mathrm{g\ C\ m^{-2}\ yr^{-1}}$). The simulated rate during the HTM was 26.5 $\mathrm{g\ C\ m^{-2}\ yr^{-1}}$, up to five times higher than the rest of the Holocene (5.04 $\mathrm{g\ C\ m^{-2}\ yr^{-1}}$). This corresponded to the observed average rate of 20 $\mathrm{C\ m^{-2}\ yr^{-1}}$ from 11.5 to 8.6 ka, which is, four times higher than 5 $\mathrm{C\ m^{-2}\ yr^{-1}}$ over the rest of the Holocene.

3.2 Vegetation Carbon

Model simulations showed an overall low vegetation C before the HTM (15-11 ka) (Figure 5a), paralleled to the relatively low annual NPP (Figure 5b). The lowest amount of C (~0.8 $\mathrm{kg\ C\ m^{-2}}$) was stored in *Sphagnum*-dominated peatland. *Sphagnum*-black spruce peatland also had low vegetation C density (~1 $\mathrm{kg\ C\ m^{-2}}$). Upland vegetation showed a generally higher C storage, among which boreal evergreen needleleaf forest ranked the first (~2 $\mathrm{kg\ C\ m^{-2}}$). Highest NPP accompanied by highest vegetation carbon appeared during the HTM (11-9 ka) (Figures 5a and b). Lower annual C uptake along with lower C was found during mid- and late-

Holocene (9 ka-19th), where peatland ecosystems exhibited the most obvious drops (Figures 5a and b).

In general, vegetation held about 2 Pg C before the HTM (Figure 6). Upland tundra ecosystems accounted for the most amount of C. During the HTM, Boreal evergreen needleleaf forest reached its highest and had an overwhelming proportion over total C. Similarly, a peak of total vegetation C appeared at the same time, averaging around 4.3 Pg C. Large decrease occurred at the mid-Holocene and a slight decline continued till the late-Holocene. We estimated a total 2.9 Pg C stored in modern Alaskan vegetation, with 0.4 Pg in peatlands and 2.5 Pg in non-peatlands. The uncertainties during the model calibration (Table 4) resulted in 0.3-0.6 Pg C and 2.2-3.1 Pg C in peatlands (see Wang et al. (2016) for model parameters) and non-peatland vegetation (see Tang and Zhuang (2008) for uncertainty analyses for upland vegetation), respectively. Our estimation of 2.5-3.7 Pg C stored in the Alaskan vegetation was lower than the previous estimate of 5 Pg (Balshi et al., 2007; McGuire et al., 2009), presumably due to the prior ranges of model parameters used from Tang and Zhuang (2008). Our overestimation of peatland area may also lead to a reduction of Alaskan non-peatland area.

3.3 Soil Carbon

Carbon storage in Alaskan non-peatland soils varied spatially (Figure 7). Moist tundra had the highest SOC density (12-25 kg $\mathrm{C\ m^{-2}}$), followed by deciduous broadleaf forest (8-13 kg $\mathrm{C\ m^{-2}}$) and evergreen needleleaf forest (3-8 kg $\mathrm{C\ m^{-2}}$) through all time slices between 15 ka and 2000 AD. Dramatic changes of vegetation types have occurred in Alaska during different periods (Figure 2). Before the HTM (15-11 ka), the terrestrial ecosystem was dominated by tundra. Northwestern coast and eastern interior was covered by moist tundra. Southwestern Alaska and the interior south of the Brooks Range were dominated by alpine tundra (Figure 2a). The basal ages of peat samples from Gorham et al. (2012) suggested that peatlands were likely to form from the (alpine) tundra ecosystems, although patches of boreal deciduous broadleaf forest and boreal evergreen needleleaf and mixed forest appeared at the north of the Alaska Range. Initially, only *Sphagnum* open peatland (SP) existed, with less C (<10 kg $\mathrm{C\ m^{-2}}$) sequestrated in the southeastern Brooks Range in comparison with southwestern and northwestern coastal parts (>15 kg $\mathrm{C\ m^{-2}}$) (Figure 8a). Approximately 4.5×10^5 $\mathrm{km^2}$ area was covered by peatlands at the beginning of the HTM (~11 ka) (Figure 9). During the HTM (11-9 ka), boreal deciduous broadleaf and boreal evergreen needleleaf and mixed forests expanded (Figures 8b and c). Coastal tundra (moist wet tundra) covered north of the Brooks Range between 11 and 10 ka, where SP continued its expansion (Figure 8b). *Sphagnum*-black spruce forested peatland began forming in southwestern coast and eastern interior regions, with a rapid increase of total peatland area to about 13×10^5 $\mathrm{km^2}$ (Figure 9). At 10-9 ka, boreal deciduous forest expanded to north of the Brooks Range, making forest the dominant biome in Alaska (Figure 2c). Prevailing forest ecosystems indicated a large expansion of peatland, with SBP covering the interior Alaska (Figure 8c). During the mid-Holocene (9-5 ka), the terrestrial landscape generally resembled present-day ecosystems (Bigelow et al., 2003). Boreal evergreen needleleaf and mixed forest prevailed in southern and interior Alaska with tundra returned to north of the Brooks Range and western Alaska (Figures 2d and e). Although SP kept forming towards west, some areas dominated by SBP in interior Alaska ceased accumulating C (Figure 8d). At 5k-19$^{\mathrm{th}}$, almost all the peatlands have formed, with some interior regions exhibiting a C loss (Figure 8e). C accumulation increased again in the last century, averaging about 20 kg $\mathrm{C\ m^{-2}\ kyr^{-1}}$ (Figure 8f).

We found that the distribution of SOC densities of both upland and peatland varied greatly depending on the vegetation distribution within each time slice, indicating that vegetation composition might be a major factor controlling regional C dynamics.

An average peat SOC "apparent" accumulation rate of 13 $\mathrm{g\ C\ m^{-2}yr^{-1}}$ (2.3 Tg C $\mathrm{yr^{-1}}$ for the entire Alaska) was estimated from 15 ka to 2000 AD (Figure 10), lower than 18.6 $\mathrm{g\ C\ m^{-2}yr^{-1}}$ as estimated from peat cores for northern peatlands (Yu et al., 2010), and slightly higher than the observed rate of 13.2 $\mathrm{g\ C\ m^{-2}yr^{-1}}$ from four peatlands in Alaska (Jones and Yu, 2010). A simulated peak occurred during the HTM with the rate 29.1 $\mathrm{g\ C\ m^{-2}yr^{-1}}$ (5.1 Tg C $\mathrm{yr^{-1}}$), which was slightly higher than the observed 25 $\mathrm{g\ C\ m^{-2}yr^{-1}}$ for northern peatlands and ~20 $\mathrm{g\ C\ m^{-2}yr^{-1}}$ for Alaska (Yu et al., 2010). It was almost four times higher than the rate 6.9 $\mathrm{g\ C\ m^{-2}yr^{-1}}$ (1.4 Tg C $\mathrm{yr^{-1}}$) over the rest of the Holocene, which corresponded to the peat core-based observations of ~5 $\mathrm{g\ C\ m^{-2}yr^{-1}}$. The mid- and late Holocene showed much slower C accumulation at a rate approximately five folds lower than during the HTM. This corresponded to the observation of a six-fold decrease in the rate of new peatland formation after 8.6 ka (Jones and Yu 2010). The C accumulation rates increased abruptly to 39.2 $\mathrm{g\ C\ m^{-2}yr^{-1}}$during the last century, within the field-measured average apparent rate range of 20-50 $\mathrm{g\ C\ m^{-2}yr^{-1}}$ over the last 2000 years (Yu et al., 2010).

The SOC stock of northern peatlands has been estimated in many studies, ranging from 210 to 621 Pg (Oechel 1989; Gorham 1991; Armentano and Menges, 1986; Turunen et al., 2002; Yu et al., 2010; see Yu 2012 for a review). Assuming Alaskan peatlands were representative of northern peatlands and using the area of Alaskan peatlands ($0.45 \times 10^6\ \mathrm{km^2}$; Kivinen and Pakarinen, 1981) divided by the total area of northern peatlnads (~$4 \times 10^6\ \mathrm{km^2}$; Maltby and

Immirzi 1993), we estimated a SOC stock of 23.6-69.9 Pg C for Alaskan peatlands. Our model estimated 27-48 Pg C (23.9 Pg C in SP and 13.5 Pg C in SBP) had been accumulated from 15 ka to 2000 AD (Figure 11), due to uncertain parameters (Table 4, see Wang et al. (2016) for model parameters). The uncertainty can also be resulted from peat basal age distributions and the estimation of total peatland area using modern inundation data as discussed above. By incorporating the observed basal age distribution to determine the expansion of peatland through time, we estimated that approximately 68% of Alaskan peatlands had formed by the end of the HTM, similar to the estimation from observed basal peat ages that 75% peatlands have formed by 8.6 ka (Jones and Yu 2010).

The northern circumpolar soils were estimated to cover approximately 18.78×10^6 km^2 (Tarnocai et al., 2009). The non-peatland soil C stock was estimated to be in the range of 150-191 Pg C for boreal forests (Apps et al., 1993; Jobbagy and Jackson, 2000), and 60-144 Pg C for tundra in the 0-100 cm depth (Apps et al., 1993; Gilmanov and Oechel, 1995; Oechel et al., 1993). 1.24×10^6 km^2 non-peatland area was estimated from the total land area of Alaska (1.69×10^6 km^2). Therefore, Alaska non-peatland soil contained 17-27 Pg C by using the ratio of Alaskan over northern non-peatland. In comparison, we modeled 9-15 Pg C (within 1-meter depth), depending on the prior ranges of model parameters from Tang and Zhuang (2008).

The simulated modern SOC distribution (Figure 12c) was largely consistent with the study of Hugelius et al. (2014) (see Figure 3 in the paper). The model captured the SOC density on northern and southwestern coasts of Alaska with most grids >40 kg C m^{-2} on average. Those regions also showed high SOC density (>75 kg C m^{-2}), which was also exhibited in our result. East part and west coast had the lowest SOC densities, corresponding to the simulation result that most grids had SOC values between 20 and 40 kg C m^{-2}. We estimated an average peat depth of

1.9 ± 0.8 m considering the uncertainties within dry bulk densities. It was similar to the observed mean depth of 2.29 m for Alaskan peatlands (Gorham et al., 1991, 2012). Our estimates (Figure 12d) showed a relatively high correlation with the 64 observed peat samples, especially with higher depths (Figure 13) ($R^2 = 0.45$). The large intercept of the regression line (101 cm) suggested that the model might have not performed well in estimating the grids with low peat depths (<50 cm). The peat characteristics (e.g., bulk density) from location to location may differ largely, even if within the same small region. Thus, it is difficult to capture the observed variations of peat depths as we used the averaged bulk density of whole Alaska.

3.4 Effects of Climate on Ecosystem Carbon Accumulation

The simulated climate by ECBilt-CLIO model showed that among the six time periods, the coolest temperature appeared at 15-11 ka, followed by the mid- and late- Holocene (5 ka-1900 AD). Those two periods were also generally dry (Figure 3f). The former represented colder and drier climate before the onset of the Holocene and the HTM (Barber and Finney, 2000; Edwards et al., 2001). The latter represented post-HTM neoglacial cooling, which has caused permafrost aggradation across northern high latitudes (Oksanen et al., 2001; Zoltai, 1995).

The simulated NPP, vegetation C density and storage were highest during the HTM. Annual C accumulation rates also reached the highest (Figures 5-11). The variation of NPP has a similar pattern of the climate (see Figure 3 for climate variables), where higher NPP, along with higher vegetation C coincided with warmer temperatures and enhanced precipitation during the HTM, compared to other time periods. ECBilt-CLIO simulated a warmest summer and a prolonged growing season, leading to a stronger seasonality of temperature during the HTM (Kaufman et al., 2004, 2016), in line with the orbitally-induced maximum summer insolation

(Berger and Loutre, 1991; Renssen et al., 2009). The coincidence between the highest vegetation C uptake and SOC accumulation rates and the warmest summer and the wetter-than-before conditions indicated a strong link between those climate variables and C dynamics in Alaska. Enhanced climate seasonality characterized by warmer summer, enhanced summer precipitation and possibly earlier snow melt during the HTM accelerated the photosynthesis and subsequently increased NPP (Tucker et al., 2001; Kimball et al., 2004; Linderholm, 2006). As shown in our sensitivity test, annual NPP was increased by 40 and 20 $\mathrm{g\ C\ m^{-2}\ yr^{-1}}$ under the warmer and wetter scenarios, respectively (Figures 14a, b). Meanwhile, warmer condition could positively affect the SOC decomposition (Nobrega et al., 2007). However, it could be offset to a certain extent via the hydrological effect, as higher precipitation could raise the water-table position, allowing less space for aerobic heterotrophic respiration. Our sensitivity test results indicated that warmer and wetter conditions could lead to an increase of decomposition up to 35 and 15 $\mathrm{g\ C\ m^{-2}\ yr^{-1}}$, respectively (Figures 14c, d). We did not find a decrease in total heterotrophic respiration throughout Alaska from the higher precipitation. It was presumably due to a much larger area of upland soils ($1.3 \times 10^6\ \mathrm{km^2}$) than peatland soils ($0.26 \times 10^6\ \mathrm{km^2}$), as higher precipitation would cause higher aerobic respiration in the unsaturated zone of upland soils, and consequently stimulated the SOC decomposition. The relatively low NPP and vegetation C density, along with the lower total soil C stocks were consistent with the unfavorable cool and dry climate conditions at 15-11 ka and during the mid- and late- Holocene. Statistical analysis indicated that temperature had the most significant effect on peat SOC accumulation rate, followed by the seasonality of NIRR (Wang et al., 2016). The seasonality of temperature, the interaction of temperature and precipitation, and precipitation alone also showed significance. The strong link between climate factors and C dynamics may explain the lower SOC accumulation during the neoglacier cooling period (Marcott et al., 2013; Vitt et al., 2000; Peteet et al., 1998; Yu et al. 2010). The rapid peat SOC accumulation during the 20th century under warming and wetter climate may suggest a continuous C sink in this century, as concluded in Spahni et al. (2013). However, the rising temperature in the future may have positive effects on heterotrophic respiration and simultaneously increase evapotranspiration and lower water table. This could increase aerobic decomposition and thus switch the Alaskan peatland from a C sink into a C source. Moreover, the increasing anthropogenic activities including land use will probably increase drought and subsequently enhance the risk of fire, releasing carbon to the atmosphere. The fate of Alaskan SOC stock and the biogeochemical cycling of the terrestrial ecosystems under future scenarios need further investigation.

3.5 Effects of Vegetation Distribution on Ecosystem Carbon Accumulation

Climate variables significantly affect C dynamics within each time slice. However, different vegetation distributions during various periods led to clear step changes, suggesting vegetation composition was likely to be another primary factor (Figures 6, 7, 8, and 11). As key parameters controlling C dynamics in the model (e.g., maximum rate of photosynthesis, litter fall C, maximum rate of monthly NPP) are ecosystem type specific, vegetation distribution changes may drastically affect regional plant productivity and C storage. Our sensitivity test indicated that by replacing all vegetation types with forests, there was a total increase of 36.9 Pg in upland plus peatland soils. There was also an increase of 48.8 Pg C under warmer and wetter conditions, suggesting that both climate and vegetation distribution may have played important roles in carbon accumulation.

The vegetation changes reconstructed from fossil pollen data during different time periods followed the general climate history during the last 15,000 years. For instance, the migration of dark boreal forests over snow-covered tundra during the HTM was probably induced by the warmer and wetter climate resulted from the insolation changes (He et al., 2014). The cooler and drier climate after the mid-Holocene limited the growth of boreal broadleaf conifers (Prentice et al., 1992), and therefore resulted in the replacement of broadleaf forest with needleleaf forest and tundra ecosystems. Since the parameters of our model for individual vegetation type were static, parameterizing the model using modern site-level observations might have introduced uncertainty to parameters, which may result in regional simulation uncertainties. Assuming each parameter as constant (e.g. the lowest water-table boundary, see Wang et al. (2016) for details) over time may also weaken the model's response to different climate scenarios. Furthermore, applying static vegetation maps at millennial scales and using modern elevation and pH data may simplify the complicated changes of landscape and terrestrial ecosystems, as vegetation can shift within hundreds of years (Ager and Brubake, 1985; see He et al. (2014) discussion section). Relatively coarse spatial resolution (0.5° ×0.5°) in P-TEM simulations may also introduce uncertainties. In addition, because we used the modern inundation map to delineate the peatland and upland within each grid cell, we might have overestimated the total peatland area since not all inundated areas are peatlands. Linking field-estimated basal ages of peat cores to the vegetation types during each period involves large uncertainties due to the limitation of the peat classification and insufficient peat samples. Thus, the estimated spatially explicit basal age data shall also introduce a large uncertainty to our regional quantification of carbon accumulation.

4. Conclusions

We used a biogeochemistry model for both peatland and non-peatland ecosystems to quantify the C stock and its changes over time in Alaskan terrestrial ecosystems during the last 15,000 years. The simulated peat SOC accumulation rates were compared with peat-core data from four peatlands on the Kenai Peninsula in southern Alaska. The model well estimated the peat SOC accumulation rates trajectory throughout the Holocene. Our regional simulation showed that 36-63 Pg C had been accumulated in Alaskan land ecosystems since 15,000 years, including 27-48 Pg C in peatlands and 9-15 Pg C in non-peatlands (within 1 m depth). We also estimated that 2.5-3.7 Pg C was stored in contemporary Alaskan vegetation, with 0.3-0.6 Pg C in peatlands and 2.2-3.1 Pg C in non-peatlands. The estimated average rate of peat C accumulation was 2.3 Tg C yr^{-1} with a peak (5.1 Pg C yr^{-1}) in the Holocene Thermal Maximum (HTM), four folds higher than the rate of 1.4 Pg C yr^{-1} over the rest of the Holocene. The 20^{th} century represented another high SOC accumulation period after a much low accumulation period of the late Holocene. We estimated an average depth of 1.9 m of peat in current Alaskan peatlands, similar to the observed mean depth. We found that the changes of vegetation distribution were the key factor to the spatial variations of SOC accumulation in different time periods. The warming in the HTM characterized by the increased summer temperature and increased seasonality of solar radiation, along with the higher precipitation might have played an important role in the high C accumulation.

5. Acknowledgment. We acknowledge the funding support from a NSF project IIS-1027955 and a DOE project DE-SC0008092. We also acknowledge the SPRUCE project to allow us use its data. Data presented in this paper are publicly accessible: ECBilt-CLIO Paleosimulation (http://apdrc.soest.hawaii.edu/datadoc/sim2bl.php), CRU2.0 (http://www.cru.uea.ac.uk/data). Model parameter data and model evaluation process are in Wang et al. (2016). Other simulation

data including model codes are available upon request from the corresponding author (qzhuang@purdue.edu).

6. References

Ager, T. A., & Brubaker, L.: Quaternary palynology and vegetational history of Alaska. Pollen Records of Late Quaternary North American Sediments, 353-384, 1985.

Apps, M. J., Kurz, W. A., Luxmoore, R. J., Nilsson, L. O., Sedjo, R. A., Schmidt, R., ... & Vinson, T. S.: Boreal forests and tundra. Water, Air, and Soil Pollution, 70(1-4), 39-53, 1993.

Armentano, T. V., & Menges, E. S.: Patterns of change in the carbon balance of organic soil-wetlands of the temperate zone. The Journal of Ecology, 755-774, 1986.

Assessment, A. C. I.: Forests, land management and agriculture.Arctic Climate Impact Assessment, 781-862, 2005.

Balshi, M. S., McGuire, A. D., Zhuang, Q., Melillo, J., Kicklighter, D. W., Kasischke, E., ... & Burnside, T. J.: The role of historical fire disturbance in the carbon dynamics of the pan-boreal region: A process-based analysis. Journal of Geophysical Research: Biogeosciences, 112(G2), 2007.

Barber, V. A., & Finney, B. P.: Late Quaternary paleoclimatic reconstructions for interior Alaska based on paleolake-level data and hydrologic models. Journal of Paleolimnology, 24(1), 29-41, 2000.

Belyea, L. R.: Nonlinear dynamics of peatlands and potential feedbacks on the climate system. Carbon cycling in northern peatlands, 5-18, 2009.

Berger, A., & Loutre, M. F.: Insolation values for the climate of the last 10 million years. Quaternary Science Reviews, 10(4), 297-317, 1991.

Bigelow, N. H., Brubaker, L. B., Edwards, M. E., Harrison, S. P., Prentice, I. C., Anderson, P. M., ... & Kaplan, J. O.: Climate change and Arctic ecosystems: 1. Vegetation changes north of 55 N between the last glacial maximum, mid-Holocene, and present. Journal of Geophysical Research: Atmospheres, 108(D19), 2003.

Bridgham, S. D., Megonigal, J. P., Keller, J. K., Bliss, N. B., & Trettin, C.: The carbon balance of North American wetlands. Wetlands, 26(4), 889-916, 2006.

Carter, A. J., & Scholes, R. J.: SoilData v2. 0: generating a global database of soil properties. Environmentek CSIR, Pretoria, South Africa, 2000.

Change, I. C.: Mitigation of Climate Change. Contribution of Working Group III to the Fifth Assessment Report of the Intergovernmental Panel on Climate Change. Cambridge University Press, Cambridge, UK and New York, NY, 2014.

Change, I. C.: The Physical Science Basis: Working Group I Contribution to the Fifth Assessment Report of the Intergovernmental Panel on Climate Change. New York: Cambridge University Press, 1, 535-1, 2013.

Chivers, M. R., Turetsky, M. R., Waddington, J. M., Harden, J. W., & McGuire, A. D.: Effects of experimental water table and temperature manipulations on ecosystem CO2 fluxes in an Alaskan rich fen.Ecosystems, 12(8), 1329-1342, 2009.

Churchill, A.: The response of plant community structure and productivity to changes in hydrology in Alaskan boreal peatlands. Master Thesis, University of Alaska, Fairbanks, AK, USA. 119 pp, 2011.

Conrad, R.: Contribution of hydrogen to methane production and control of hydrogen concentrations in methanogenic soils and sediments.FEMS Microbiology Ecology, 28(3), 193-202, 1999.

Davidson, E. A., & Janssens, I. A.: Temperature sensitivity of soil carbon decomposition and feedbacks to climate change. Nature, 440(7081), 165-173, 2006.

Davidson, E. A., Trumbore, S. E., & Amundson, R.: Biogeochemistry: soil warming and organic carbon content. Nature, 408(6814), 789-790, 2000.

Edwards, M. E., Mock, C. J., Finney, B. P., Barber, V. A., & Bartlein, P. J.: Potential analogues for paleoclimatic variations in eastern interior Alaska during the past 14,000 yr: atmospheric-circulation controls of regional temperature and moisture responses. Quaternary Science Reviews, 20(1), 189-202, 2001.

Euskirchen, E. S., McGuire, A. D., & Chapin, F. S.: Energy feedbacks of northern high-latitude ecosystems to the climate system due to reduced snow cover during 20th century warming. Global Change Biology,13(11), 2425-2438, 2007.

Frolking, S., Roulet, N. T., Tuittila, E., Bubier, J. L., Quillet, A., Talbot, J., & Richard, P. J. H.: A new model of Holocene peatland net primary production, decomposition, water balance, and peat accumulation. Earth System Dynamics, 1(1), 1-21, 2010.

Frolking, S., Talbot, J., Jones, M. C., Treat, C. C., Kauffman, J. B., Tuittila, E. S., & Roulet, N.: Peatlands in the Earth’s 21st century climate system. Environmental Reviews, 19(NA), 371-396, 2011.

Gilmanov, T. G., & Oechel, W. C.: New estimates of organic matter reserves and net primary productivity of the North American tundra ecosystems. Journal of Biogeography, 723-741, 1995.

Gorham, E. V. I. L. L. E.: Biotic impoverishment in northern peatlands. The earth in transition: patterns and processes of biotic impoverishment. Cambridge University Press, Cambridge, UK, 65-98, 1990.

Gorham, E., Lehman, C., Dyke, A., Clymo, D., & Janssens, J.: Long-term carbon sequestration in North American peatlands. Quaternary Science Reviews, 58, 77-82, 2012.

Gorham, E.: Northern peatlands: role in the carbon cycle and probable responses to climatic warming. Ecological applications, 1(2), 182-195, 1991.

He, Y., Jones, M. C., Zhuang, Q., Bochicchio, C., Felzer, B. S., Mason, E., & Yu, Z.: Evaluating CO 2 and CH 4 dynamics of Alaskan ecosystems during the Holocene Thermal Maximum. Quaternary Science Reviews, 86, 63-77, 2014.

Hinzman, L. D., Viereck, L. A., Adams, P. C., Romanovsky, V. E., & Yoshikawa, K.: Climate and permafrost dynamics of the Alaskan boreal forest. Alaska’s Changing Boreal Forest, 39-61, 2006.

Hobbie, S. E.: Interactions between litter lignin and nitrogenitter lignin and soil nitrogen availability during leaf litter decomposition in a Hawaiian montane forest. Ecosystems, 3(5), 484-494, 2000.

Hugelius, G., Strauss, J., Zubrzycki, S., Harden, J. W., Schuur, E., Ping, C. L., ... & O'Donnell, J. A.: Estimated stocks of circumpolar permafrost carbon with quantified uncertainty ranges and identified data gaps.Biogeosciences, 11(23), 6573-6593, 2014.

Jobbágy, E. G., & Jackson, R. B.: The vertical distribution of soil organic carbon and its relation to climate and vegetation. Ecological applications, 10(2), 423-436, 2000.

Jones, M. C., & Yu, Z.: Rapid deglacial and early Holocene expansion of peatlands in Alaska. Proceedings of the National Academy of Sciences,107(16), 7347-7352, 2010.

Jones, P. D., & Moberg, A.: Hemispheric and large-scale surface air temperature variations: An extensive revision and an update to 2001. Journal of Climate, 16(2), 206-223, 2003.

Kane, E. S., Turetsky, M. R., Harden, J. W., McGuire, A. D., & Waddington, J. M.: Seasonal ice and hydrologic controls on dissolved organic carbon and nitrogen concentrations in a boreal-rich fen. Journal of Geophysical Research: Biogeosciences, 115(G4), 2010.

Kaufman, D. S., Ager, T. A., Anderson, N. J., Anderson, P. M., Andrews, J. T., Bartlein, P. J., ... & Dyke, A. S.: Holocene thermal maximum in the western Arctic (0–180 W). Quaternary Science Reviews, 23(5), 529-560, 2004.

Kaufman, D.S., Axford, Y.L., Henerson, A., McKay, N.P., Oswald, W.W., Saenger, C., Anderson, R.S., Bailey, H.L., Clegg, B., Gajewski, K., Hu, F.S., Jones, M.C., Massa, C., Routson, C.C., Werner, A., Wooller, M.J., Yu, Z.: Holocene climate changes in eastern Beringia (NW North America) e a systemic review of multi-proxy evidence. Quaternary Science Reviews, this volume. http://dx.doi.org/10.1016/ j.quascirev.2015.10.021, 2016.

Keller, J. K., & Bridgham, S. D.: Pathways of anaerobic carbon cycling across an ombrotrophic–minerotrophic peatland gradient, 2007.

Keller, J. K., & Takagi, K. K.: Solid-phase organic matter reduction regulates anaerobic decomposition in bog soil. Ecosphere, 4(5), 1-12, 2013.

Kimball, J. S., McDonald, K. C., Running, S. W., & Frolking, S. E.: Satellite radar remote sensing of seasonal growing seasons for boreal and subalpine evergreen forests. Remote Sensing of Environment, 90(2), 243-258, 2004.

Kivinen, E., and P. Pakarinen.: Geographical distribution of peat resources and major peatland complex types in the world. Annales Academiae Scientarum Fennicae, Series A, Number 132, 1981.

Kleinen, T., Brovkin, V., & Schuldt, R. J.: A dynamic model of wetland extent and peat accumulation: results for the Holocene.Biogeosciences, 9(1), 235-248, 2012.

Kuhry, P., & Vitt, D. H.: Fossil carbon/nitrogen ratios as a measure of peat decomposition. Ecology, 77(1), 271-275, 1996.

Linderholm, H. W.: Growing season changes in the last century.Agricultural and Forest Meteorology, 137(1), 1-14, 2006.

Loisel, J., Gallego-Sala, A. V., & Yu, Z.: Global-scale pattern of peatland Sphagnum growth driven by photosynthetically active radiation and growing season length. Biogeosciences, 9(7), 2737-2746, 2012.

Loisel, J., Yu, Z., Beilman, D. W., Camill, P., Alm, J., Amesbury, M. J., ... & Belyea, L. R.: A database and synthesis of northern peatland soil properties and Holocene carbon and nitrogen accumulation. the Holocene, 0959683614538073, 2014.

Maltby, E., & Immirzi, P.: Carbon dynamics in peatlands and other wetland soils regional and global perspectives. Chemosphere, 27(6), 999-1023, 1993.

Manabe, S., & Wetherald, R. T.: On the distribution of climate change resulting from an increase in CO2 content of the atmosphere. Journal of the Atmospheric Sciences, 37(1), 99-118, 1980.

Manabe, S., & Wetherald, R. T.: Reduction in summer soil wetness induced by an increase in atmospheric carbon dioxide. Science, 232(4750), 626-628, 1986.

Marcott, S. A., Shakun, J. D., Clark, P. U., & Mix, A. C.: A reconstruction of regional and global temperature for the past 11,300 years.science, 339(6124), 1198-1201, 2013.

Matthews, E., & Fung, I.: Methane emission from natural wetlands: Global distribution, area, and environmental characteristics of sources.Global biogeochemical cycles, 1(1), 61-86, 1987.

McGuire, A. D., & Hobbie, J. E.: Global climate change and the equilibrium responses of carbon storage in arctic and subarctic regions. InModeling the Arctic system: A workshop report on the state of modeling in the Arctic System Science program, pp. 53-54, 1997.

McGuire, A. D., Anderson, L. G., Christensen, T. R., Dallimore, S., Guo, L., Hayes, D. J., ... & Roulet, N.: Sensitivity of the carbon cycle in the Arctic to climate change. Ecological Monographs, 79(4), 523-555, 2009.

McGuire, A. D., Melillo, J. M., Kicklighter, D. W., & Joyce, L. A.: Equilibrium responses of soil carbon to climate change: empirical and process-based estimates. Journal of Biogeography, 785-796, 1995.

Melillo, J. M., Kicklighter, D. W., McGuire, A. D., Peterjohn, W. T., & Newkirk, K.: Global change and its effects on soil organic carbon stocks. In Dahlem Conference Proceedings, John Wiley and Sons, New York, John Wiley & Sons, Ltd., Chichster, pp. 175-189, 1995.

Mitchell, T. D., Carter, T. R., Jones, P. D., Hulme, M., & New, M.: A comprehensive set of high-resolution grids of monthly climate for Europe and the globe: the observed record (1901–2000) and 16 scenarios (2001–2100).Tyndall centre for climate change research working paper, 55(0), 25, 2004.

Moore, T. R., Bubier, J. L., Frolking, S. E., Lafleur, P. M., & Roulet, N. T.: Plant biomass and production and CO2 exchange in an ombrotrophic bog. Journal of Ecology, 90(1), 25-36, 2002.

Nobrega, S., & Grogan, P.: Deeper snow enhances winter respiration from both plant-associated and bulk soil carbon pools in birch hummock tundra. Ecosystems, 10(3), 419-431, 2007.

Oechel, W. C., Hastings, S. J., Vourlrtis, G., Jenkins, M., Riechers, G., & Grulke, N.: Recent change of Arctic tundra ecosystems from a net carbon dioxide sink to a source. Nature, 361(6412), 520-523, 1993.

Oechel, W. C.: Nutrient and water flux in a small arctic watershed: an overview. Holarctic Ecology, 229-237, 1989.

Oksanen, P. O., Kuhry, P., & Alekseeva, R. N.: Holocene development of the Rogovaya river peat plateau, European Russian Arctic.The Holocene, 11(1), 25-40, 2001.

Peteet, D., Andreev, A., Bardeen, W., & Mistretta, F.: Long-term Arctic peatland dynamics, vegetation and climate history of the Pur-Taz region, western Siberia. Boreas, 27(2), 115-126, 1998.

Prentice, I. C., Cramer, W., Harrison, S. P., Leemans, R., Monserud, R. A., & Solomon, A. M.: Special paper: a global biome model based on plant physiology and dominance, soil properties and climate. Journal of biogeography, 117-134, 1992.

Raich, J. W., Rastetter, E. B., Melillo, J. M., Kicklighter, D. W., Steudler, P. A., Peterson, B. J., ... & Vorosmarty, C. J.: Potential net primary productivity in South America: application of a global model. Ecological Applications, 1(4), 399-429, 1991.

Renssen, H., Seppä, H., Heiri, O., Roche, D. M., Goosse, H., & Fichefet, T.: The spatial and temporal complexity of the Holocene thermal maximum. Nature Geoscience, 2(6), 411-414, 2009.

Roulet, N. T., Lafleur, P. M., Richard, P. J., Moore, T. R., Humphreys, E. R., & Bubier, J. I. L. L.: Contemporary carbon balance and late Holocene carbon accumulation in a northern peatland. Global Change Biology, 13(2), 397-411, 2007.

Saarinen, T.: Biomass and production of two vascular plants in a boreal mesotrophic fen. Canadian Journal of Botany, 74(6), 934-938, 1996.

Schuur, E. A., Bockheim, J., Canadell, J. G., Euskirchen, E., Field, C. B., Goryachkin, S. V., ... & Mazhitova, G.: Vulnerability of permafrost carbon to climate change: implications for the global carbon cycle.BioScience, 58(8), 701-714, 2008.

Sitch, S., Smith, B., Prentice, I. C., Arneth, A., Bondeau, A., Cramer, W., ... & Thonicke, K.: Evaluation of ecosystem dynamics, plant geography and terrestrial carbon cycling in the LPJ dynamic global vegetation model.Global Change Biology, 9(2), 161-185, 2003.

Spahni, R., Joos, F., Stocker, B. D., Steinacher, M., & Yu, Z. C.: Transient simulations of the carbon and nitrogen dynamics in northern peatlands: from the Last Glacial Maximum to the 21st century. Climate of the Past, 9(3), 1287-1308, 2013.

Stocker, B. D., Spahni, R., & Joos, F.: DYPTOP: a cost-efficient TOPMODEL implementation to simulate sub-grid spatio-temporal dynamics of global wetlands and peatlands. Geoscientific Model Development, 7(6), 3089-3110, 2014.

Stocker, B. D., Strassmann, K., & Joos, F.: Sensitivity of Holocene atmospheric CO 2 and the modern carbon budget to early human land use: analyses with a process-based model. Biogeosciences, 8(1), 69-88, 2011.

Tang, J., & Zhuang, Q.: A global sensitivity analysis and Bayesian inference framework for improving the parameter estimation and prediction of a process-based Terrestrial Ecosystem Model. Journal of Geophysical Research: Atmospheres, 114(D15), 2009.

Tang, J., & Zhuang, Q.: Equifinality in parameterization of process-based biogeochemistry models: A significant uncertainty source to the estimation of regional carbon dynamics. Journal of Geophysical Research: Biogeosciences, 113(G4), 2008.

Tang, J., Zhuang, Q., Shannon, R. D., & White, J. R.: Quantifying wetland methane emissions with process-based models of different complexities. Biogeosciences, 7(11), 3817-3837, 2010.

Tarnocai, C., Canadell, J. G., Schuur, E. A. G., Kuhry, P., Mazhitova, G., & Zimov, S.: Soil organic carbon pools in the northern circumpolar permafrost region. Global biogeochemical cycles, 23(2), 2009.

Timm, O., & Timmermann, A.: Simulation of the Last 21 000 Years Using Accelerated Transient Boundary Conditions*. Journal of Climate,20(17), 4377-4401, 2007.

Tucker, C. J., Slayback, D. A., Pinzon, J. E., Los, S. O., Myneni, R. B., & Taylor, M. G.: Higher northern latitude normalized difference vegetation index and growing season trends from 1982 to 1999. International journal of biometeorology, 45(4), 184-190, 2001.

Turetsky, M. R., Treat, C. C., Waldrop, M. P., Waddington, J. M., Harden, J. W., & McGuire, A. D.: Short-term response of methane fluxes and methanogen activity to water table and soil warming manipulations in an Alaskan peatland. Journal of Geophysical Research: Biogeosciences,113(G3), 2008.

Turunen, J., Tomppo, E., Tolonen, K., & Reinikainen, A.: Estimating carbon accumulation rates of undrained mires in Finland–application to boreal and subarctic regions. The Holocene, 12(1), 69-80, 2002.

Vitt, D. H., Halsey, L. A., Bauer, I. E., & Campbell, C.: Spatial and temporal trends in carbon storage of peatlands of continental western Canada through the Holocene. Canadian Journal of Earth Sciences, 37(5), 683-693, 2000.

Wang, S., Zhuang, Q., Yu, Z., Bridgham, S., & Keller, J. K.: Quantifying peat carbon accumulation in Alaska using a process-based biogeochemistry model, Journal of Geophysical Research: Biogeosciences., 121, doi: 10.1002/2016JG003452, 2016.

XU-RI and PRENTICE, I. C.: Terrestrial nitrogen cycle simulation with a dynamic global vegetation model. Global Change Biology, 14: 1745–1764. doi:10.1111/j.1365-2486.2008.01625.x, 2008.

Yu, Z. C.: Northern peatland carbon stocks and dynamics: a review. Biogeosciences, 9(10), 4071-4085, 2012.

Yu, Z., Beilman, D. W., & Jones, M. C.: Sensitivity of northern peatland carbon dynamics to Holocene climate change. Carbon cycling in northern peatlands, 55-69, 2009.

Yu, Z., Loisel, J., Brosseau, D. P., Beilman, D. W., & Hunt, S. J.: Global peatland dynamics since the Last Glacial Maximum. Geophysical Research Letters, 37(13), 2010.

Zhuang, Q., McGuire, A. D., Melillo, J. M., Clein, J. S., Dargaville, R. J., Kicklighter, D. W., ... & Hobbie, J. E.: Carbon cycling in extratropical terrestrial ecosystems of the Northern Hemisphere during the 20th century: a modeling analysis of the influences of soil thermal dynamics. Tellus B, 55(3), 751-776, 2003.

Zhuang, Q., McGuire, A. D., O'neill, K. P., Harden, J. W., Romanovsky, V. E., & Yarie, J.: Modeling soil thermal and carbon dynamics of a fire chronosequence in interior Alaska. Journal of Geophysical Research: Atmospheres, 107(D1), 2002.

Zhuang, Q., Melillo, J. M., Kicklighter, D. W., Prinn, R. G., McGuire, A. D., Steudler, P. A., ... & Hu, S.: Methane fluxes between terrestrial ecosystems and the atmosphere at northern high latitudes during the past century: A retrospective analysis with a process-based biogeochemistry model. Global Biogeochemical Cycles, 18(3), 2004.

Zhuang, Q., Melillo, J. M., McGuire, A. D., Kicklighter, D. W., Prinn, R. G., Steudler, P. A., ... & Hu, S.: Net emissions of CH4 and CO2 in Alaska: Implications for the region's greenhouse gas budget. Ecological Applications, 17(1), 203-212, 2007.

Zhuang, Q., Romanovsky, V. E., & McGuire, A. D.: Incorporation of a permafrost model into a large-scale ecosystem model: Evaluation of temporal and spatial scaling issues in simulating soil thermal dynamics.Journal of Geophysical Research: Atmospheres, 106(D24), 33649-33670, 2001.

Zhuang, Q., Zhu, X., He, Y., Prigent, C., Melillo, J. M., McGuire, A. D., ... & Kicklighter, D. W.: Influence of changes in wetland inundation extent on net fluxes of carbon dioxide and methane in northern high latitudes from 1993 to 2004. Environmental Research Letters, 10(9), 095009, 2015.

Zimov, S. A., Schuur, E. A., & Chapin III, F. S.: Permafrost and the global carbon budget. Science(Washington), 312(5780), 1612-1613, 2006.

Zoltai, S. C.: Permafrost distribution in peatlands of west-central Canada during the Holocene warm period 6000 years BP. Géographie physique et Quaternaire, 49(1), 45-54, 1995.

Table 1. Description of sites and variables used for parameterizing the core carbon and nitrogen module (CNDM).

Site[a]	Vegetation	Observed variables for CNDM parameterization	References
APEXCON	Moderate rich open fen with sedges (*Carex* sp.), spiked rushes (*Eleocharis* sp.), *Sphagnum* spp., and brown mosses (e.g., *Drepanocladus aduncus*)	Mean annual aboveground NPP in 2009; Mean annual belowground NPP in 2009; Aboveground biomass in 2009	Chivers et al. (2009) Turetsky et al. (2008) Kane et al. (2010) Churchill et al. (2011)
APEXPER	Peat plateau bog with black spruce (*Picea mariana*), *Sphagnum* spp., and feather mosses		

[a]The Alaskan Peatland Experiment (APEX) site is adjacent to the Bonanza Creek Experimental Forest (BCEF) site, approximately 35 km southwest of Fairbanks, AK. The area is classified as continental boreal climate with a mean annual temperature of -2.9℃ and annual precipitation of 269 mm, of which 30% is snow (Hinzman et al., 2006).

Table 2. Carbon pools and fluxes used for calibration of CMDM

Annual Carbon Fluxes or Pools[a]	*Sphagnum* Open Fen		*Sphagnum*-Black Spruce Bog		References
	Observation	Simulation	Observation	Simulation	
NPP	445 ± 260	410	433 ± 107	390	Turetsky et al. (2008), Churchill (2011)
Aboveground Vegetation Carbon	149-287		423		Saarinen et al. (1996)
Belowground Vegetation Carbon	347-669		987		Moore et al. (2002)
Total Vegetation Carbon Density	496-856	800	1410	1300	Zhuang et al. (2002)
Litter Fall Carbon Flux	300	333	300	290	Tarnocai et al. (2009)
Methane Emission Flux	19.5	19.2	9.7	12.8	Kuhry and Vitt (1996)

[a] Units for annual net primary production (NPP) and litter fall carbon are $\mathrm{g\ C\ m^{-2}\ yr^{-1}}$. Units for vegetation carbon density are $\mathrm{g\ C\ m^{-2}}$. Units for Methane emissions are $\mathrm{g\ C-CH_4\ m^{-2}\ yr^{-1}}$. The simulated total annual methane fluxes were compared with the observations at APEXCON in 2005 and SPRUCE in 2012. A ratio of 0.47 was used to convert vegetation biomass to carbon (Raich 1991).

Table 3. Assignment of biomized fossil pollen data to the vegetation types in TEM (He et al., 2014).

TEM upland vegetation	TEM peatland vegetation	BIOMISE code
Alpine tundra		CUSH DRYT PROS
Moist tundra	*Sphagnum* spp. open fen	DWAR SHRU
Boreal evergreen needleleaf and mixed forest	*Sphagnum*-black spruce bog	TAIG COCO CLMX COMX
Boreal deciduous broadleaf forest		CLDE

Table 4. Relations between peatland basal age and vegetation distribution

Peatland basal age	Vegetation types	Location in Alaska
15-11 ka	alpine tundra	south, northwestern, and southeastern coast
11-10 ka	moist tundra boreal evergreen needleleaf forest boreal deciduous broadleaf forest	south, north, and southeastern coast east central part
10-9 ka	moist tundra boreal evergreen needleleaf forest boreal deciduous broadleaf forest	south and north coast central part
9-5 ka	moist tundra boreal evergreen needleleaf forest	central part
5 ka-1900 AD	moist tundra boreal evergreen needleleaf forest	west coast

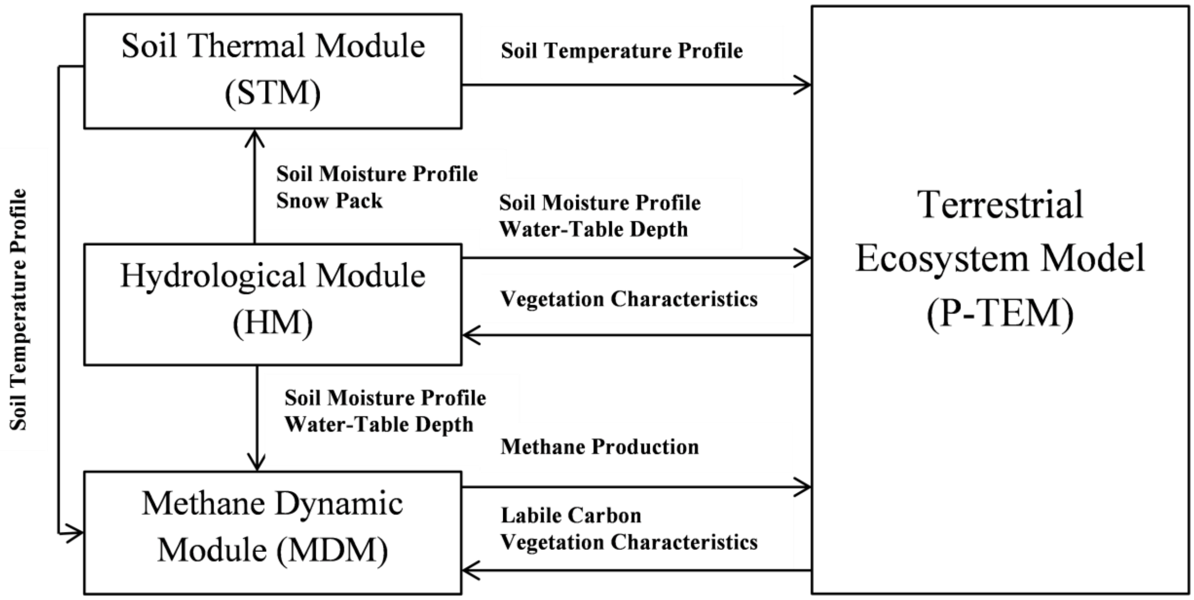

Figure 1. P-TEM (Peatland-Terrestrial Ecosystem Model) framework includes a soil thermal module (STM), a hydrologic module (HM), a carbon/ nitrogen dynamic model (CNDM), and a methane dynamics module (MDM) (Wang et al., 2016).

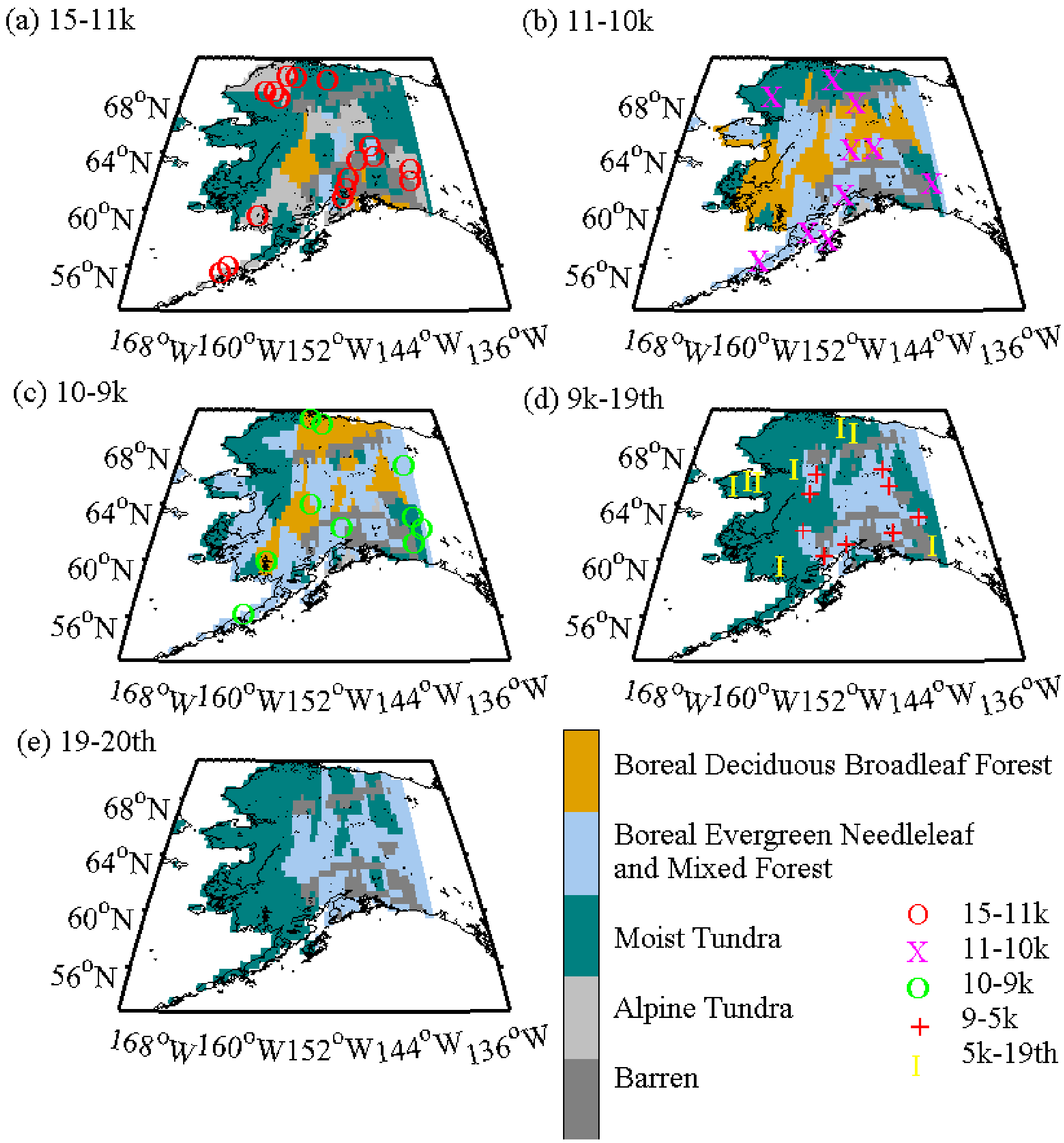

Figure 2. Alaskan vegetation distribution maps reconstructed from fossil pollen data during (a) 15-11 ka, (b) 11-10 ka, (c) 10-9 ka, (d) 9 ka -1900 AD, and (e) 1900-2000 AD (He et al., 2014). Symbols represent the basal age of peat samples (n = 102) in Gorham et al. (2012). Each symbol indicates 1-3 peat samples in the map. Peat samples with basal age 9-5k and 5k-19th are shown in map (d) as there is no change of vegetation distribution during 9k-19th. Barren refers to mountain range and large water body areas that can not be interpolated.

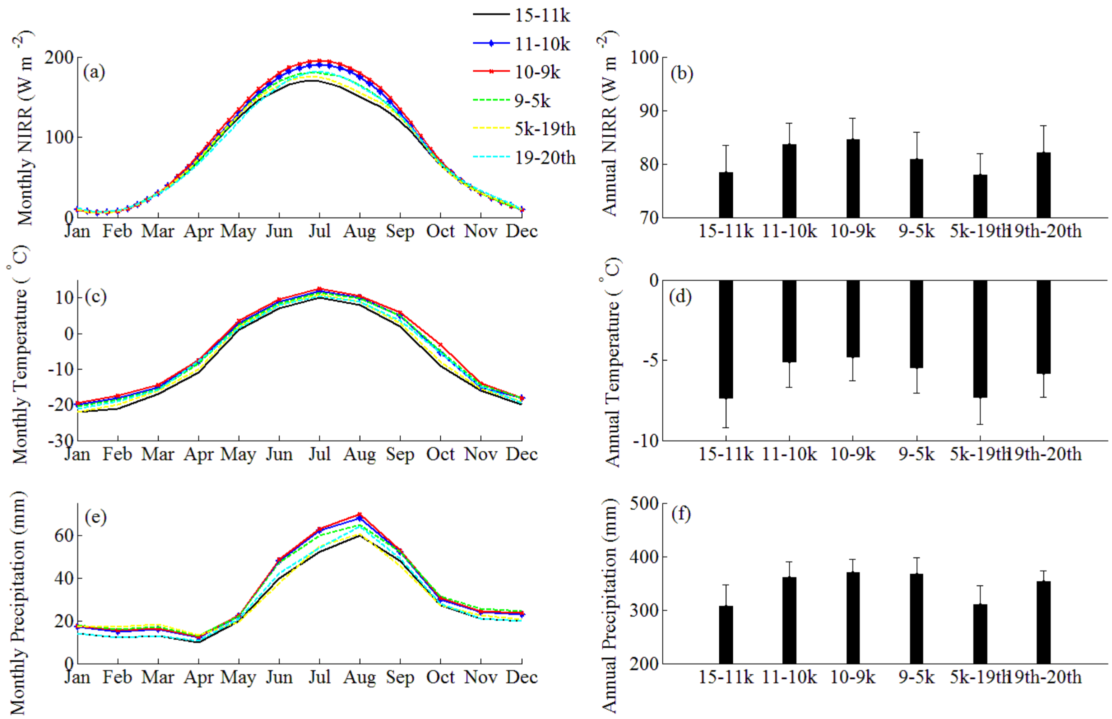

Figure 3. Simulated Paleo-climate and other input data from 15 ka to 2000 AD: (a) mean monthly and (b) mean annual net incoming solar radiation (NIRR, W m^{-2}), (c) mean monthly and (d) mean annual air temperature (℃), (e) mean monthly, and (f) mean annual precipitation (mm) (Timm and Timmermann, 2007; He et al., 2014).

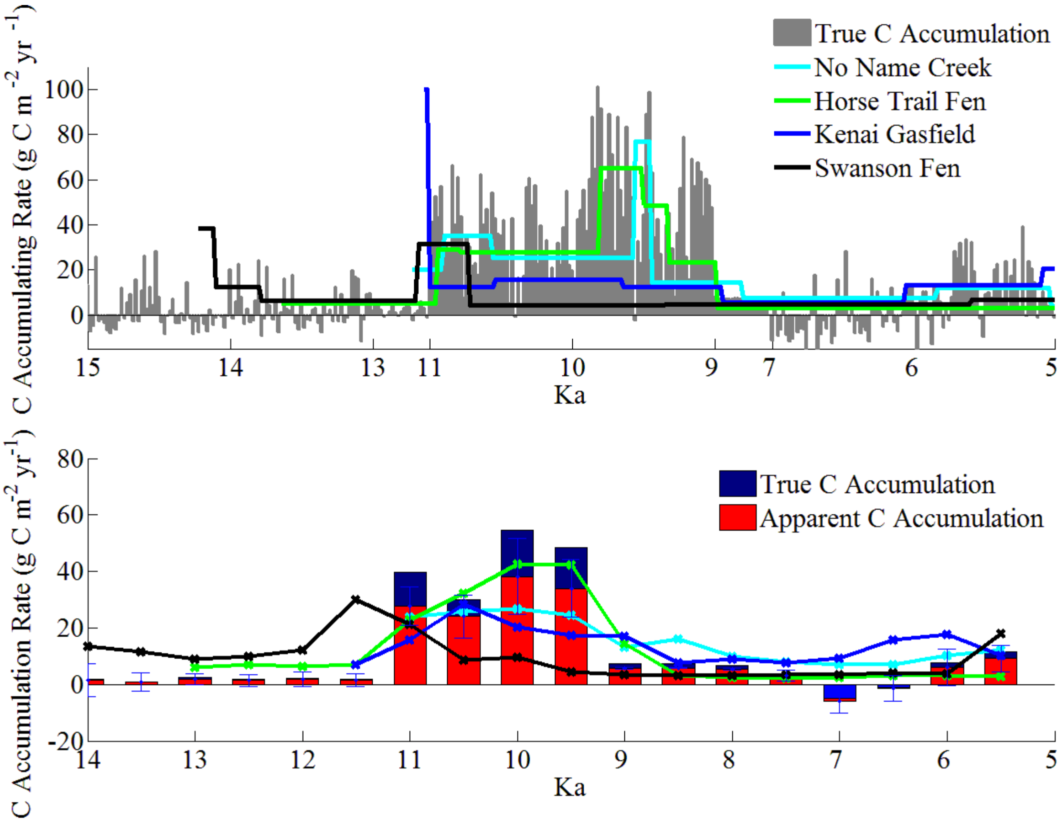

Figure 4. Simulated and observed carbon accumulation rates from 15 ka to 5 ka in 20-yr bins (a) and 500-yr bins with standard deviation (b) for No Name Creek, Horse Trail Fen, Kenai Gasfield, and Swanson Fen. Peat-core data were from Jones and Yu (2010).

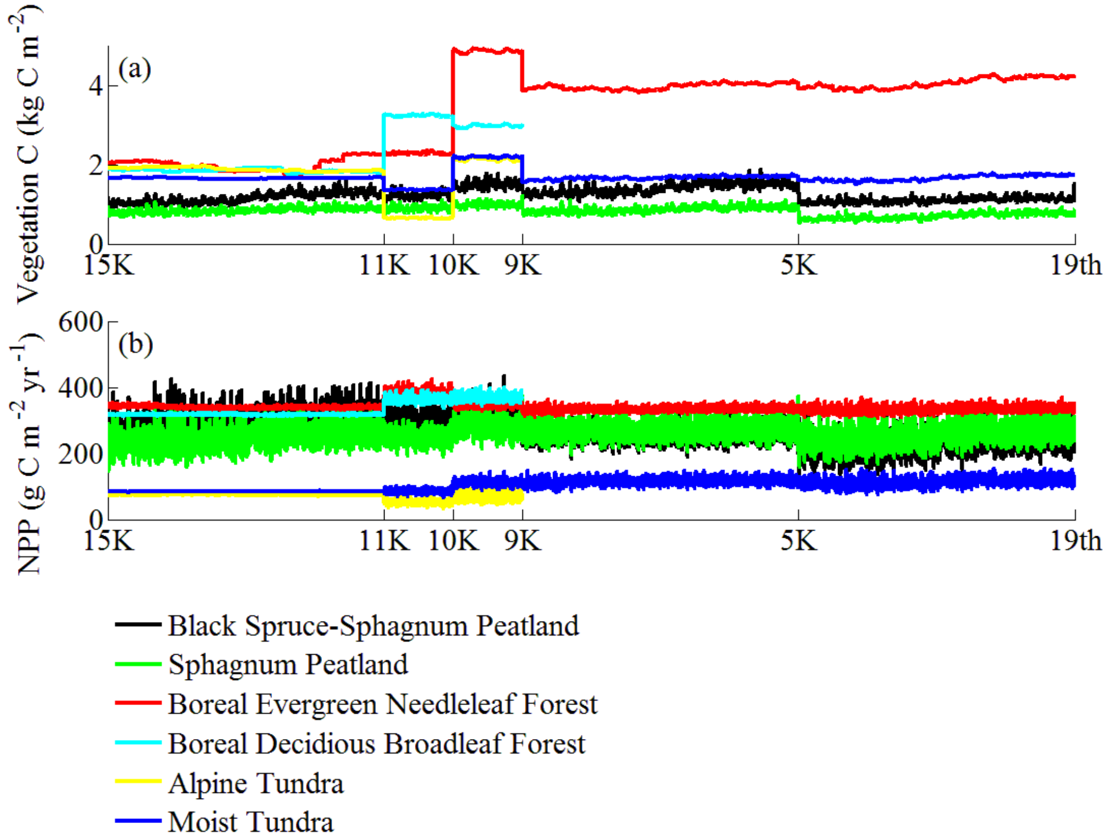

Figure 5. Simulated (a) mean vegetation carbon density (kg C m^{-2}) of different vegetation types and (b) NPP (g C $m^{-2}yr^{-1}$).

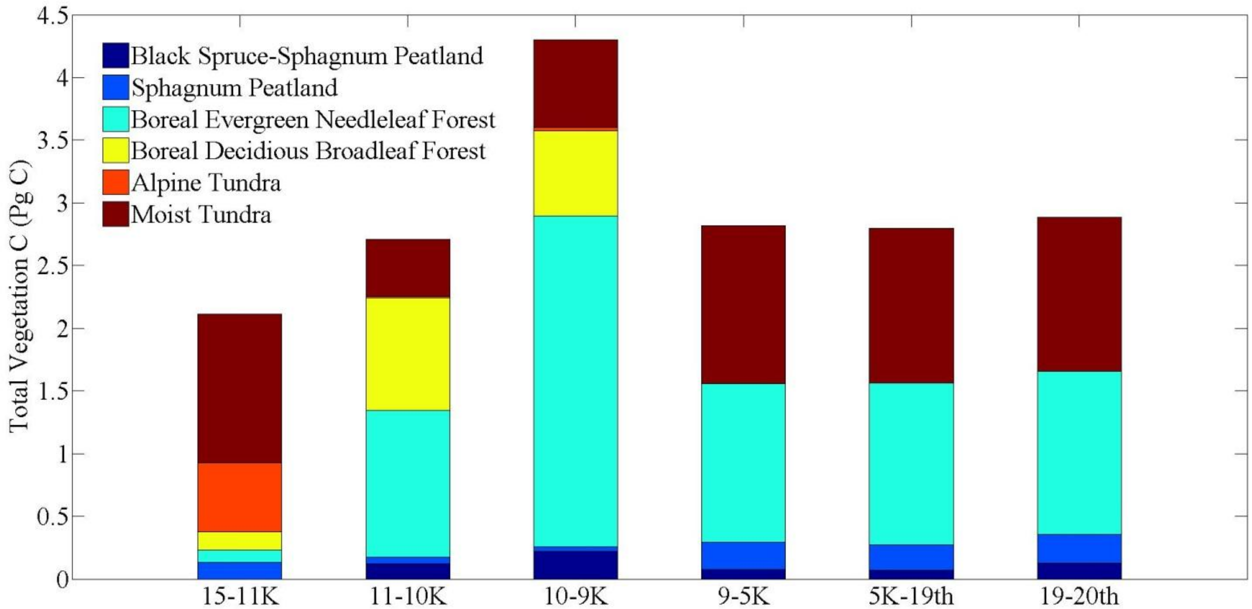

Figure 6. Total C (Pg C) stored in Alaskan vegetation for different time periods.

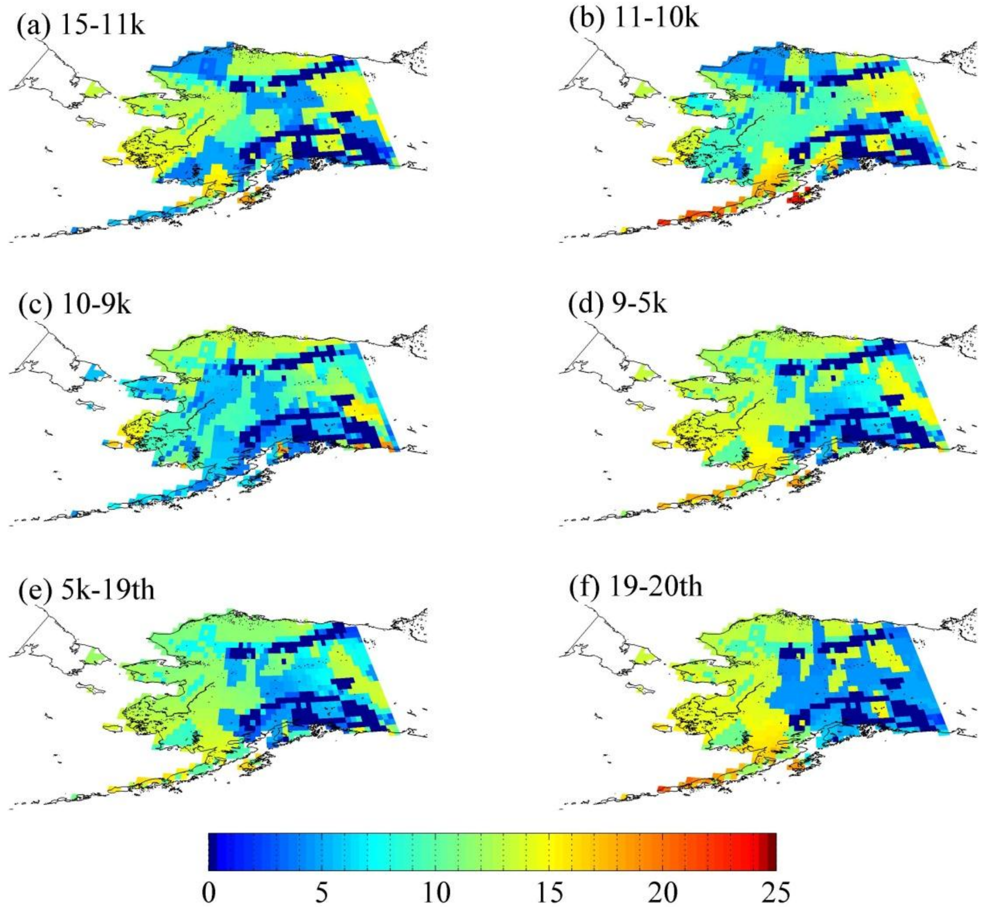

Figure 7. Average non-peatland (mineral) SOC density (kg C m^{-2}) during (a) 15-11 ka, (b) 11-10 ka, (c) 10-9 ka, (d) 9-5 ka, (e) 5 ka -1900 AD, and (f) 1900-2000 AD. The period of 9k-19th in Figure 2d is separated into 9-5k and 5k-19th.

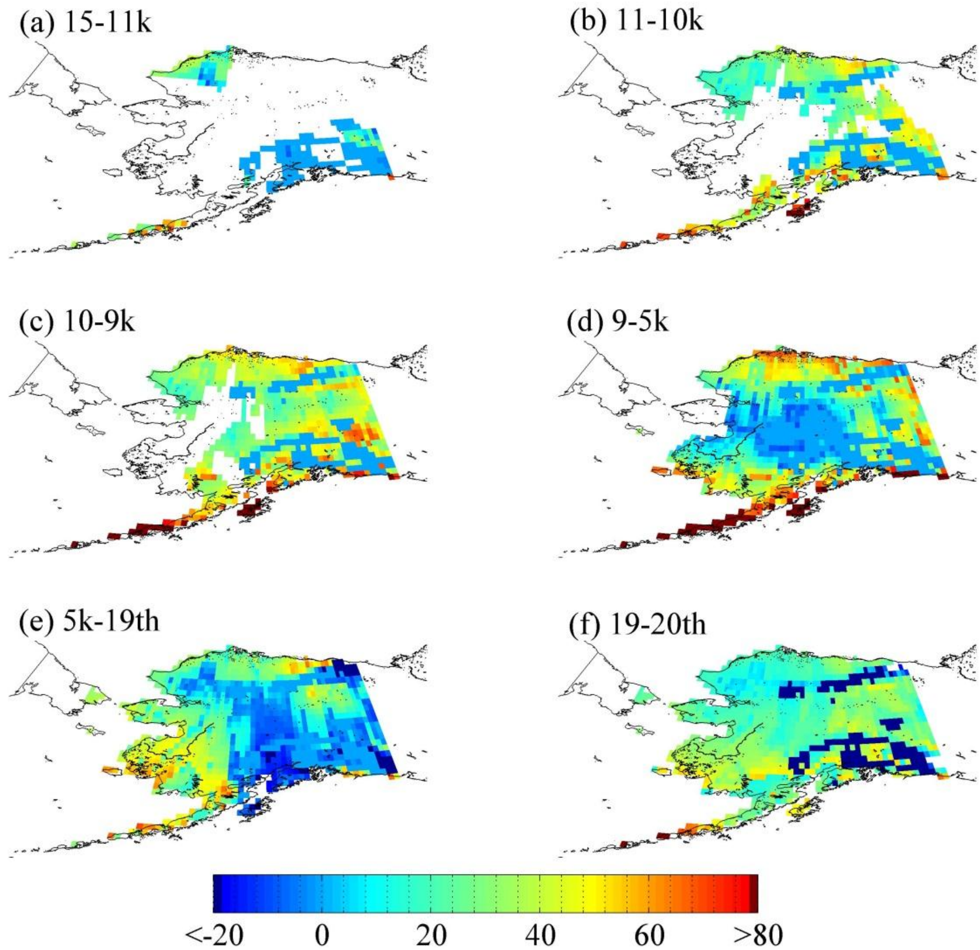

Figure 8. Peatland area expansion and peat soil C accumulation per 1000 years (kg C m^{-2} kyr^{-1}) during (a) 15-11 ka, (b) 11-10 ka, (c) 10-9 ka, (d) 9-5 ka, (e) 5 ka -1900 AD, and (f) 1900-2000 AD. The amount of C represents the C accumulation as the difference between the peat C amount in the final year and the first year in each time slice. The period of 9k-19th in Figure 2d is separated into 9-5k and 5k-19th.

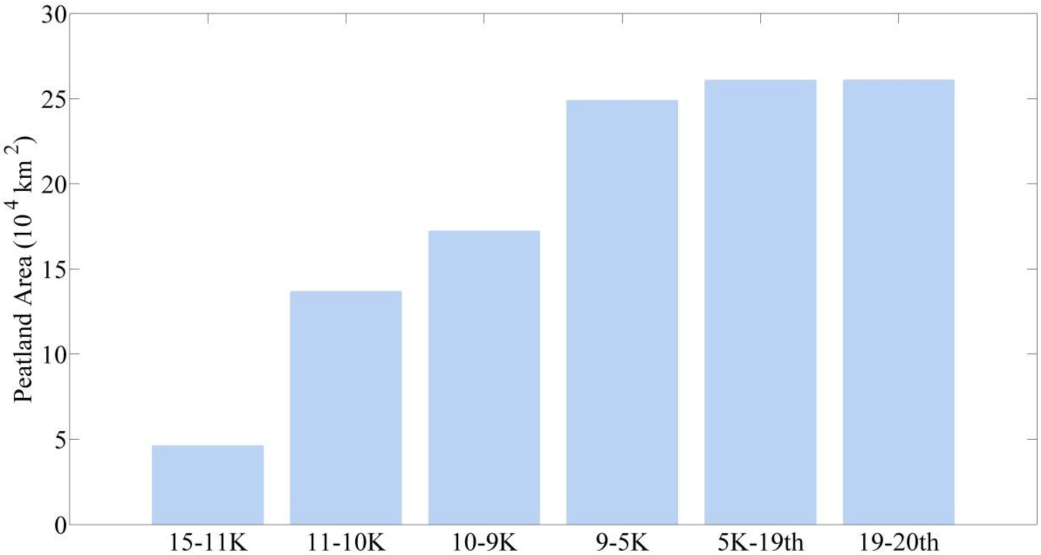

Figure 9. Peatland expansion area (10^4 km^2) in different time slices, the area of barren in the map is set to 0 km^2.

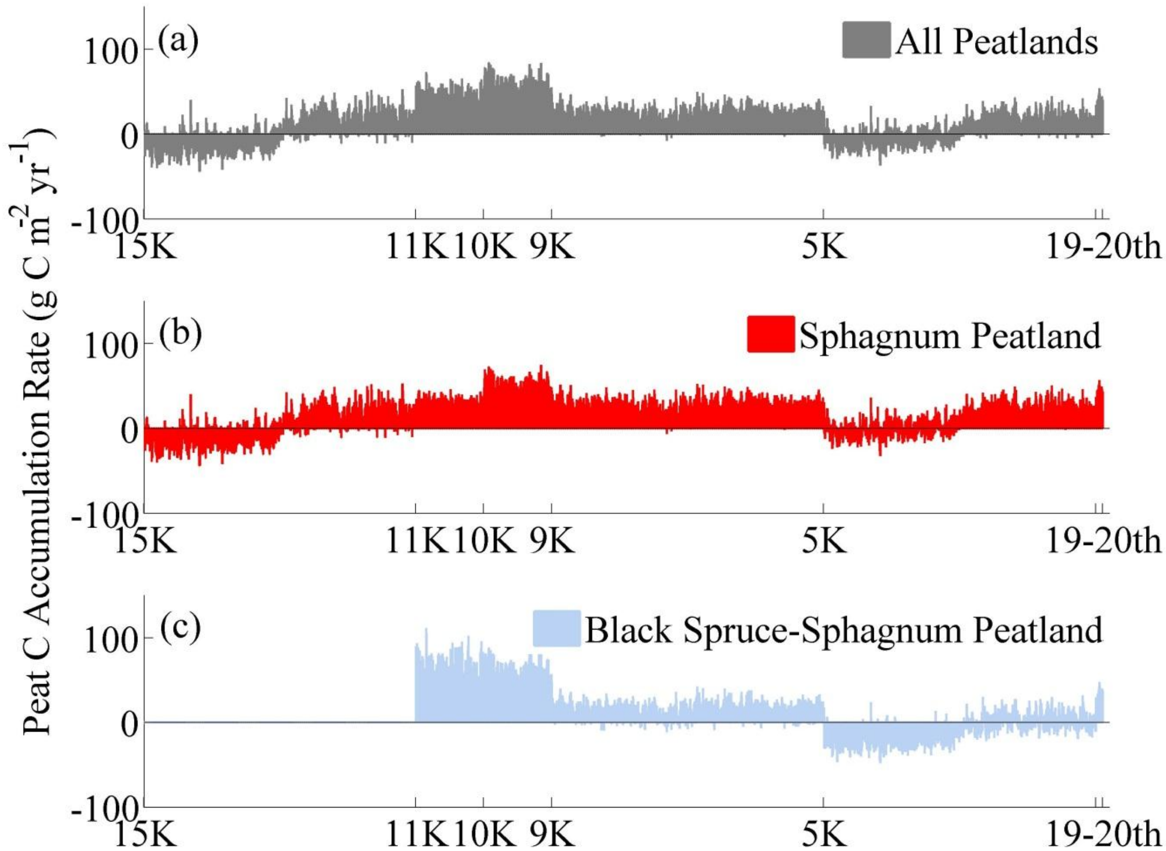

Figure 10. Peatland mean C accumulation rates from 15 ka to 2000 AD for (a) weighted average of all peatlands, (b) *Sphagnum* open peatlands, and (c) *Sphagnum*-black spruce peatlands.

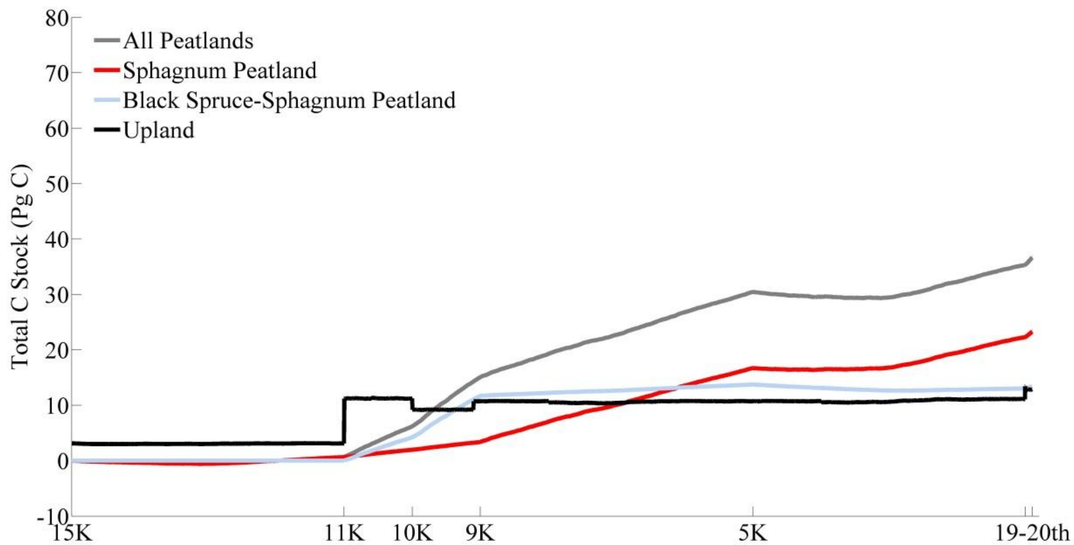

Figure 11. Total C stock accumulated from 15 ka to 2000 AD for all peatlands, *Sphagnum* open peatlands, *Sphagnum*-black spruce peatlands, and upland soils.

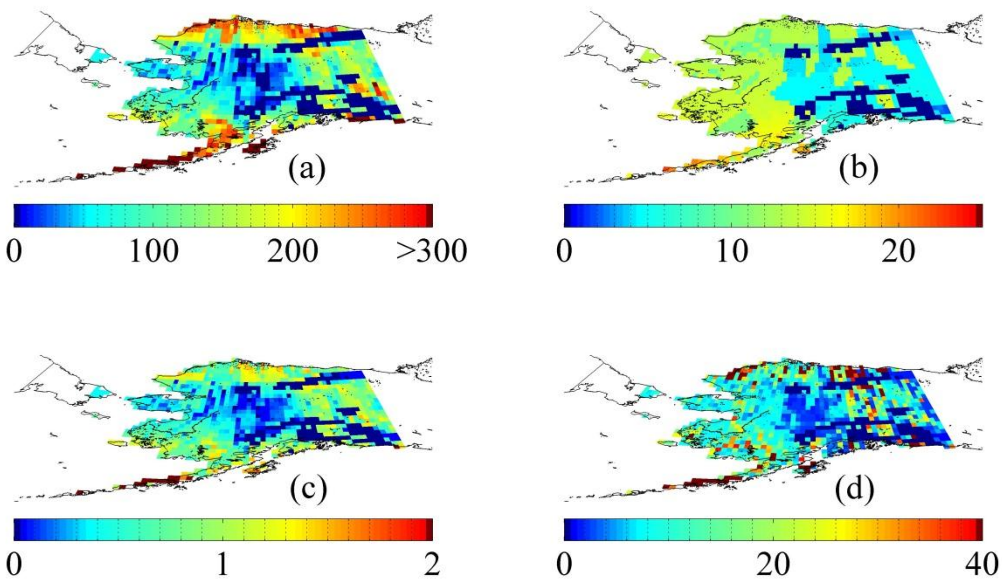

Figure 12. Spatial distribution of (a) total peat SOC density (kg C m^{-2}), (b) total mineral SOC density (kg C m^{-2}), (c) total peat depth (m), and (d) area-weighted total (peatlands plus non-peatlands) SOC density (kg C m^{-2}) in Alaska from 15 ka to 2000 AD.

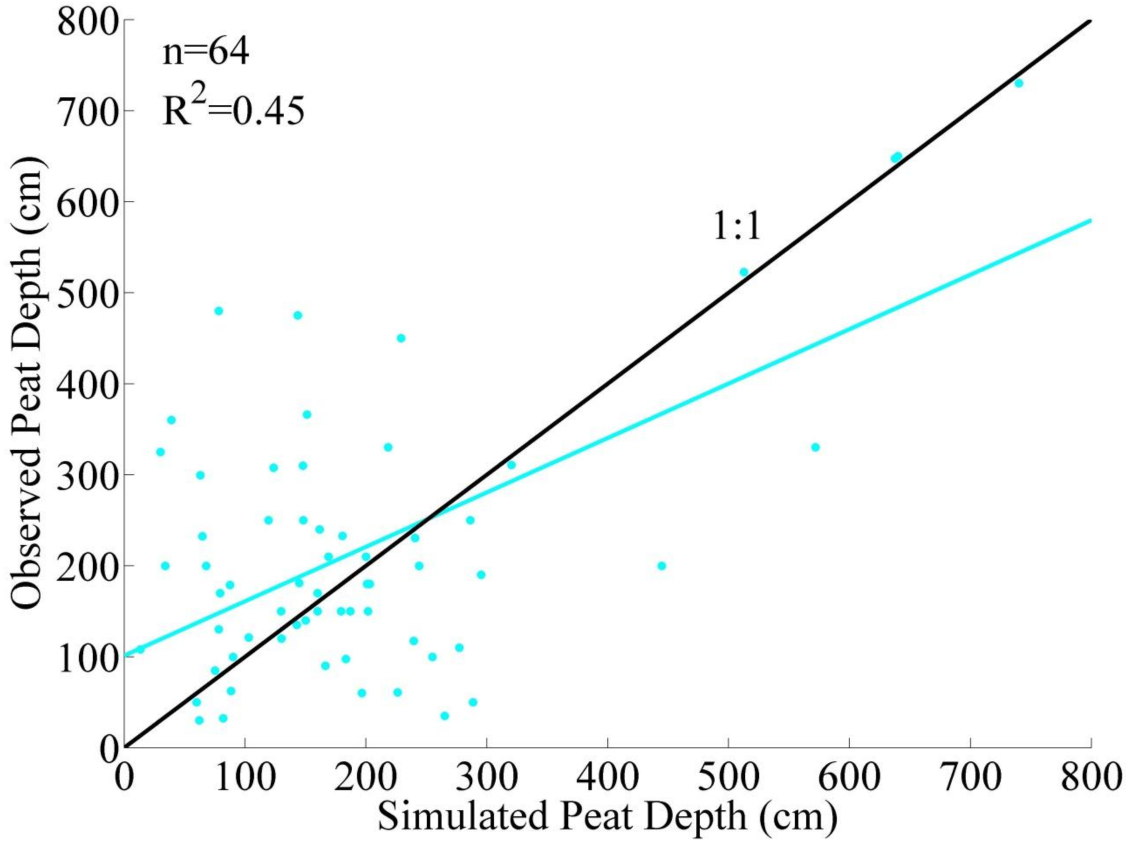

Figure 13. Field-based estimates and model simulations for peat depths in Alaska: The observed and simulated data are extracted from the same grids on the map. Linear regression line (cyan) is compared with the 1:1 line. The linear regression is significant ($P<0.001$, $n = 64$) with $R^2 = 0.45$, slope = 0.65, and intercept = 101.05 cm. The observations of >1000 cm are treated as outliers.

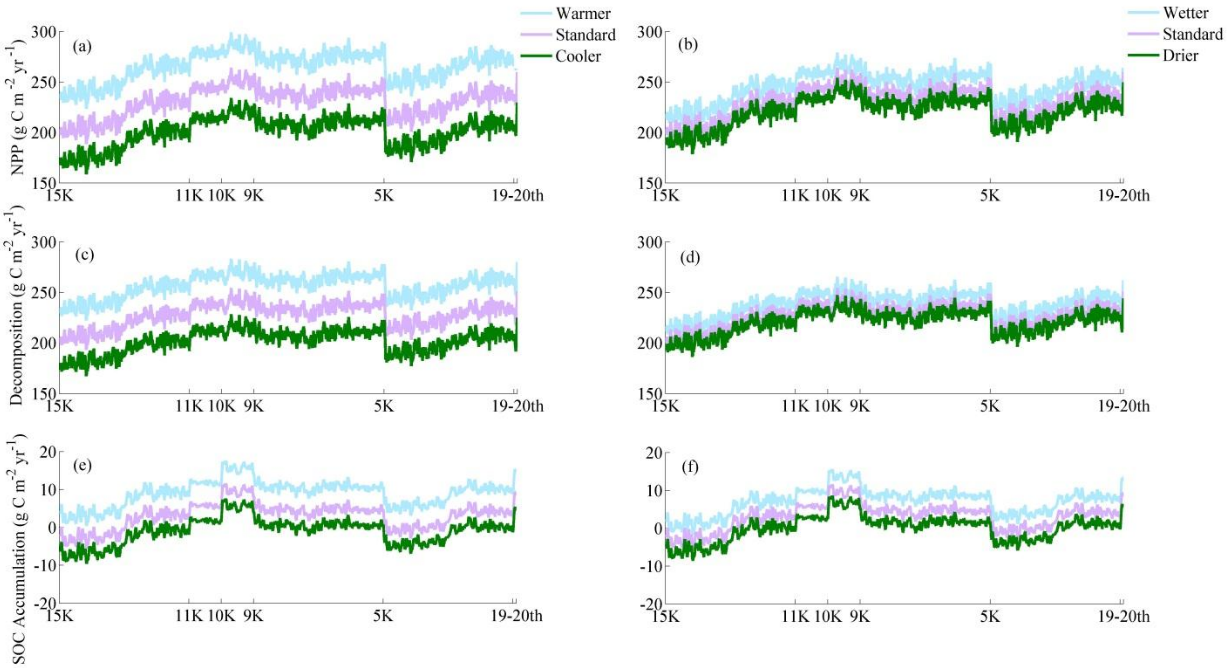

Figure 14. Temperature and precipitation effects on (a)(b) annual NPP, (c)(d) annual SOC decomposition rate (aerobic plus anaerobic), and (e)(f) annual SOC accumulation rate of Alaska. A 10-year moving average was applied.